Molecules **2014**, *19*, 11999-12010; doi:10.3390/molecules190811999

OPEN ACCESS

molecules

ISSN 1420-3049

www.mdpi.com/journal/molecules

Article

Dissociative Electron Transfer to Diphenyl-Substituted Bicyclic Endoperoxides: The Effect of Molecular Structure on the Reactivity of Distonic Radical Anions and Determination of Thermochemical Parameters

David C. Magri [1,*] and Mark S. Workentin [2,*]

[1] Department of Chemistry, University of Malta, Msida, MSD 2080, Malta

[2] Department of Chemistry, The University of Western Ontario, London, ON N6A 5B7, Canada

* Authors to whom correspondence should be addressed; E-Mails: david.magri@um.edu.mt (D.C.M.); mworkent@uwo.ca (M.S.W.); Tel.: +356-2340-2276 (D.C.M.); +519-661-2111 (ext. 86319) (M.S.W.); Fax: +356-2340-3320 (D.C.M.); +519-661-3022 (M.S.W.).

Received: 24 June 2014; in revised form: 29 July 2014 / Accepted: 1 August 2014 / Published: 11 August 2014

Abstract: The heterogeneous electron transfer reduction of the bicyclic endoperoxide 1,4-diphenyl-2,3-dioxabicyclo[2.2.1]hept-5-ene (**4**) was investigated in *N*,*N*-dimethylformamide at a glassy carbon electrode. The endoperoxide reacts by a concerted dissociative ET mechanism resulting in reduction of the O-O bond with an observed peak potential of −1.4 V at 0.2 V s^{-1}. The major product (90% yield) resulting from the heterogeneous bulk electrolysis of **4** at −1.4 V with a rotating disk glassy carbon electrode is 1,4-diphenyl-cyclopent-2-ene-*cis*-1,3-diol with a consumption of 1.73 electrons per mole. In contrast, 1,4-diphenyl-2,3-dioxabicyclo[2.2.2]oct-5-ene (**1**), undergoes a two-electron reduction mechanism in quantitative yield. This difference in product yield between **1** and **4** is suggestive of a radical-anion mechanism, as observed with 1,4-diphenyl-2,3-dioxabicyclo-[2.2.2] octane (**2**) and 1,4-diphenyl-2,3-dioxabicyclo[2.2.1]heptane (**3**). Convolution potential sweep voltammetry is used to determine unknown thermochemical parameters of **4**, including the O-O bond dissociation energy and the standard reduction potential and a comparison is made to the previously studied bicyclic endoperoxides **1**–**3** with respect to the effect of molecular structure on the reactivity of distonic radical anions.

Keywords: dissociative electron transfer; distonic radical ion; endoperoxide; convolution analysis; electrode interface; cyclic voltammetry

---

1. Introduction

Radical ions are an important class of reactive intermediate possessing dual reactivity with properties of both a radical and an ion [1]. They are involved in many crucial biological and synthetic organic chemistry processes and materials science applications [2]. Typically, they result from the transfer of a single electron to a neutral molecule to yield an intermediate possessing both a charge and radical character, or from the ionization of zwitterions or diradicals [3]. Both theoretical and experimental work has converged to provide convincing evidence that both charge and spin are important factors in the reactivity of radical ions [4–7]. Coote and her team have recently provided convincing evidence that in the gas phase a sufficiently stabilized localized radical linked by an aliphatic carbon spacer can be stabilized by a negative charge [8,9].

The heterogeneous reduction of aliphatic peroxides [10–13] and peresters [14–17] in aprotic solvents, such as acetonitrile and *N*,*N*-dimethylformamide (DMF), has been shown to occur by a dissociative electron transfer (ET) mechanism. Similarly, the heterogeneous reduction of endoperoxides has also been consistent with a dissociative ET mechanism [18–25] and including photo-initiated examples [26,27]. The first step of the mechanism involves O-O bond cleavage by ET to form a distonic radical-anion, a reactive intermediate with a spatially separated radical and anion (Equation (1)). Subsequently, the major competitive pathway is reduction of the distonic radical anion at the electrode, or in solution by an electrochemically-generated radical-anion donor, to the dialkoxide, which is protonated to yield the *cis*-diol (Equation (2)). The reduction of the distonic radical is highly favourable under electrochemical conditions as the reduction potential is much more positive than the initial reduction of the endoperoxide.

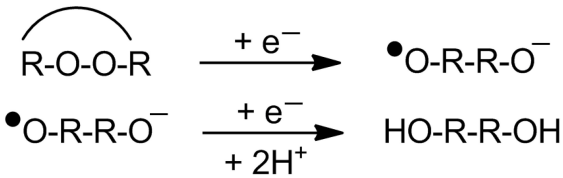

(1)

(2)

We have shown that diphenyl-substituted endoperoxides that form a distonic radical anion upon O-O cleavage may undergo a fragmentation reaction in competition with the second heterogeneous ET [18–22]. We have previously reported the ET-initiated reduction of the bicyclic endoperoxides 1,4-diphenyl-2,3-dioxabicyclo[2.2.2]oct-5-ene (**1**, Figure 1) [18], 1,4-diphenyl-2,3-dioxabicyclo[2.2.2] octane (**2**, Figure 1) [18], and 1,4-diphenyl-2,3-dioxabicyclo[2.2.1]heptane (**3**, Figure 1) [19] using heterogeneous electrochemical techniques. In these studies, we evaluated previously unknown kinetic and thermochemical data by application of Savéant's theory of dissociative ET [28–32]. With the dialkyl bicyclic endoperoxides, ascaridole and dihydroascaridole, we observed that reduction occurred by a two-electron reductive mechanism yielding the *cis*-diol in quantitative yield [22]. The same two-electron reductive mechanism was observed with the diphenyl-substituted endoperoxide (**1**). However, in the case of **2** and **3** the distonic radical anion was observed to undergo a competitive β-scission fragmentation resulting in a propagating radical-anion chain mechanism initiated by dissociative ET reduction of a bicyclic endoperoxide [18].

Figure 1. The molecular structures of bicyclic endoperoxides **1**–**4**.

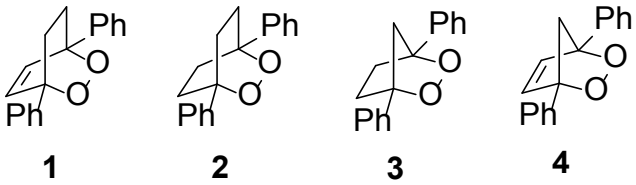

In this study we report the heterogeneous reduction of 1,4-diphenyl-2,3-dioxabicyclo[2.2.1]hept-5-ene (**4**, Figure 1) at a glassy carbon electrode. The approach is advantageous as it is relatively easy to determine the activation-driving force relationship from the obtained current-potential response. The endoperoxide was studied using a number of electrochemical techniques including cyclic voltammetry, convolution potential sweep voltammetry and preparative electrolysis in order to determine unknown thermochemical parameters, including the O-O bond dissociation energy and the standard reduction potential and to gain insight into the reactivity of the distonic radical anion resulting from cleavage of the O-O bond.

2. Results and Discussion

2.1. Cyclic Voltammetry and Constant Potential Electrolyses

The electrochemical reduction of 1,4-diphenyl-2,3-dioxabicyclo[2.2.1]hept-5-ene (**4**) was studied by cyclic voltammetry using a glassy carbon electrode in DMF containing 0.10 M tetraethylammonium perchlorate (TEAP). The voltammogram of **4**, as shown in Figure 2, is characterized by an electrochemically irreversible cathodic peak with a peak potential, E_p of −1.42 V versus SCE at 0.1 V s^{-1}. On increasing the scan rate the E_p shifts to −1.53 and −1.63 V at 1.0 and 10 V s^{-1} respectively. With increasing scan rate v the peak width at half height ($\Delta E_{p/2}$) broadens from 178 to 214 mV with a negative shift of 132 mV per log decade. The transfer coefficient α, determined from the peak widths using $\alpha = 1.857RT/(F\Delta E_p/2)$ are found to decrease with v from 0.268 to 0.223 [31]. Using the scan rate dependence of the peak potential and $\alpha = 1.15RT/[dEp/(d\log v)]$, α is 0.26 indicating the transition state closely resembles the initial reaction state. These characteristics of the voltammogram are consistent with a concerted dissociative mechanism ET mechanism. On scanning back after the forward reduction at a switching potential of −1.9 V, poorly defined anodic peaks are observed between 0.1 and −0.5 V due to oxidation of the dialkoxide anion. A summary of voltammetry data is included in Table 1 along with previous data for endoperoxides **1**–**3** for comparison. For **4** the E_p is rather similar to the other endoperoxides, whereas the $\Delta E_{p/2}$ is somewhat broader. The α values are low characteristic of an outright concerted dissociative ET mechanism.

When the switching potential is extended past the end of the initial wave, which is normally dictated exclusively by diffusion, a sharp oxidative dip is observed at −2 V. This feature of the voltammograms is most noticeable at slower scan rates yet remains visible up to 10 V s^{-1}. Following the dip at more negative scanned potentials there are other cathodic and anodic peaks attributed to products resulting from the reduction of the **4** following dissociative reduction of the O-O bond. However, the addition of excess weak acid results in an increase in peak current −2 V even at a scan rate

of 0.1 V s^{-1} (See Figure 2). These peaks are due to electroactive products resulting from the initial reduction of the O-O bond.

Figure 2. Cyclic voltammograms of 1.84 mM of **4** in a solution of DMF containing 0.10 M TEAP in the absence (solid line) and presence (dashed line) of 10 equivalents of 2,2,2-trifluoroethanol at 0.1 V s^{-1}.

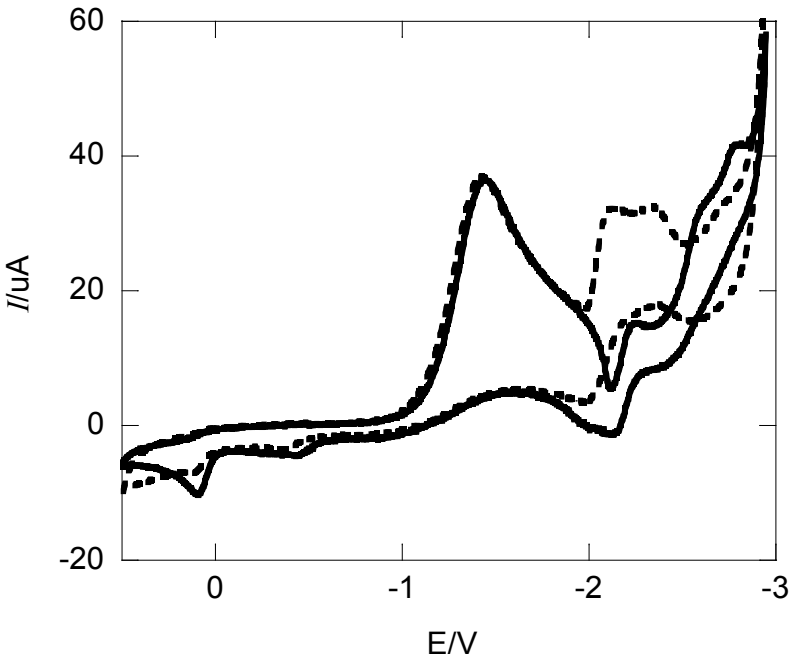

Table 1. Cyclic voltammetry data for the endoperoxides **1**–**4** in 0.10 M TEAP/DMF at 25 °C measured at a glassy carbon electrode.

Experimental CV Data	1	2	3	4
E_p/V @ 0.1 V s^{-1}	−1.27	−1.45	−1.34	−1.42
$\Delta E_{p/2}$/mV @ 0.1 V s^{-1}	136	142	116	178
α @ 0.1 V s^{-1}	0.351	0.336	0.411	0.268
$(dE_p/d\log \nu)$/mV^{-1} [a]	−118	−105	−132	−115
$\alpha = 1.15RT/F(dE_p/d\log \nu)$ [a]	0.25	0.28	0.23	0.26
n @ E_p (no acid) [b]	1.98	1.94	1.97	1.73
n @ E_p (acid) [b]	2.08	1.96	1.92	1.74
n @ E (ca. 200 mV past dip) [b]	1.96	1.3	0.8	0.8

[a] Scan rate range of 0.1 to 10 V s^{-1}. [b] Electrolyses performed with a glassy carbon rotating disc electrode.

At potentials between −1.4 to −2.0 V, between the dissociative wave and the dip, **4** consumes 1.7 F mol^{-1} of charge independent of acid present. A redox couple is observed at −2.16 V after complete disappearance of the dissociative wave, followed by other cathodic peaks at more negative potentials. The major product recovered from the electrolysis mixture in 90% yield is 1,4-diphenylcyclopent-2-ene-*cis*-1,3-diol. Electrolyses conducted at −2.2 V result in the consumption of only 0.8 F mol^{-1} of charge, and the appearance of electroactive products at more negative potentials at the expense of the dissociative wave.

2.2. Heterogeneous Kinetics and Thermochemical Parameters

The heterogeneous ET kinetics and thermochemical parameters for reduction of the O-O bond were evaluated by convolution potential sweep voltammetry [33–35]. Scan rates were varied from 0.10 to 10 V s^{-1} as observed in Figure 3a. The faster scan rates were the most reliable because of non-Cottrell behaviour at the slower scan rates. A total of 20 background-subtracted cyclic voltammograms were recorded and transformed into sigmoidal-shaped *I-E* curves by use of the convolution integral (Equation (3)) and the experimental current *i* [33–35].

$$I_{\lim} = \pi^{-1/2} \int_0^t \frac{i(u)}{(t-u)^{1/2}} du \tag{3}$$

Figure 3. (**a**) Background-subtracted linear sweep voltammograms of 2.0 mM of **4** in DMF containing 0.10 mol L^{-1} TEAP (from left to right: 0.1, 0.2, 0.4, 1.0, 2.0, 4.0, 10 V s^{-1}); (**b**) the convolution curves as a function of scan rate; (**c**) overlapping potential dependence of the log k_{het}; (**d**) the potential dependence of α_{app} at 10 scan rates between 1.0 and 20 V s^{-1}.

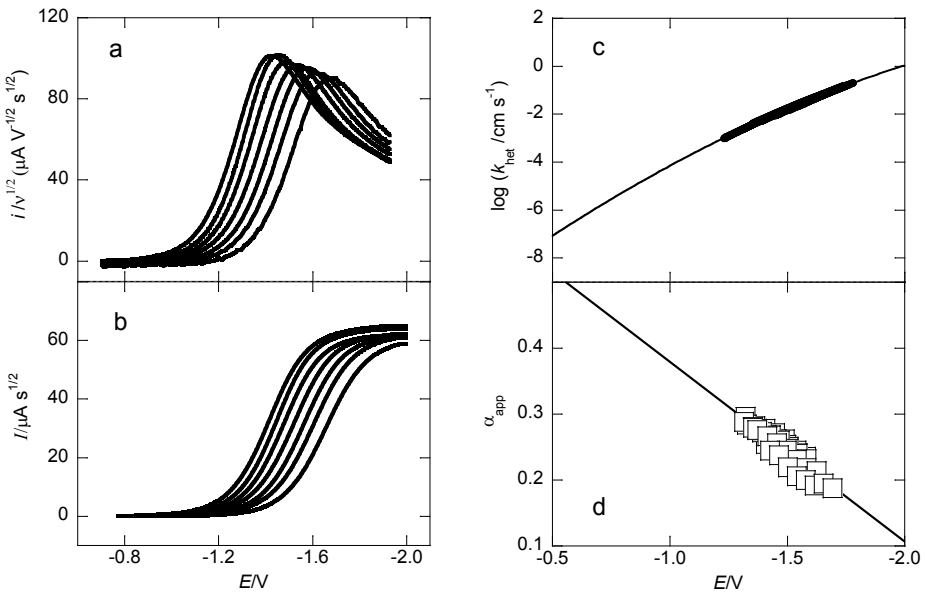

The limiting current, $I_{\lim}$, at the plateau of the sigmoidal-shaped *i-E* curves is diffusion-controlled and defined as $I_{\lim} = nFAD^{1/2}C^*$ where *n* is the overall electron consumption, *A* is the electrode area, *D* is the diffusion coefficient, and *C** is the substrate concentration. For an irreversible electrode process I_{lim} and *i* are related to k^1_{het} by:

$$\ln k^1_{het} = \ln\sqrt{D} - \ln\left(\frac{I_{\lim} - I(t)}{i(t)}\right) \tag{4}$$

Derivatisation of the ln k^1_{het} allows the evaluation of the apparent transfer coefficient, α_{app}, uncorrected for the double layer:

$$\alpha_{app} = -\left(\frac{RT}{F}\right)\frac{d\ln k^1_{het}}{dE} \tag{5}$$

The error between the limiting plateau curves was found to be within 5% (Figure 3b). From the limiting currents, I_{lim}, and the known area of the glassy carbon electrode, the diffusion coefficient in the presence of 0.1 M TEAP was determined to be 6.0×10^{-6} cm^2 s^{-1}. From the potential dependence of α_{app} for a concerted dissociative mechanism, $E°_{diss}$ was determined to be −0.56 V from extrapolation of an α_{app}-E plot corresponding to α_{app} = 0.5 (Figure 3d). The slope of the linear regression provided an intrinsic barrier of 10.6 kcal mol^{-1} (Figure 3d). The log $k°_{het}$ was evaluated to be −6.7 (Figure 3c), which is consistent with a totally irreversible rate-determining electrode reaction characteristic of concerted dissociative ET

In Table 2 the parameters from the convolution analysis are summarized along with previous results for endoperoxides **1**–**4**. As determined from the α_{app}-E plots, the evaluated $E°_{diss}$ and $\Delta G_o^{\neq}$ for **1**–**4** are consistent with average values of −0.56 V and 10.7 kcal mol^{-1}, respectively. The $E°_{diss}$ is substantially more positive than the E_p by over 0.8 V due to a large overpotential attributed to the large $\Delta G_o^{\neq}$ that must be overcome to stretch and break the O-O bond. The accuracy of the evaluated thermochemical parameters in acidic media were adequately reproduced by digital simulation of the dissociative waves using the data in Tables 1 and 2 for a two-electron concerted dissociative mechanism.

Table 2. Data acquired by convolution analysis of diphenyl-substituted bicyclic endoperoxides **1**–**4** in DMF containing 0.10 mol L^{-1} TEAP at 25 °C at a glassy carbon electrode.

Thermodynamic Data	1	2	3 [g]	4
D/cm^2 s^{-1} [a]	7.7×10^{-6}	7.4×10^{-6}	6.5×10^{-6}	6.0×10^{-6}
$E°_{diss}$/V [b]	−0.61	−0.51	−0.54	−0.56
log ($k°_{het}$/cm s^{-1}) [c]	−6.1	−6.5	−6.8	−6.7
$\Delta G_o^{\neq}$/kcal mol^{-1} [d]	9.8	10.4	11.8	10.6
λ_{het}/kcal mol^{-1} [e]	20	20	18	19
BDE/kcal mol^{-1} [f]	19	22	20 [h]	20 [i]

[a] Determined from the convoluted limiting current and the known area of the electrode. The area of the electrode was calculated using a diffusion coefficients for ferrocene of 1.13×10^{-5} cm^2 s^{-1} in DMF [11]. [b] Estimated error is ±0.10 V and uncorrected for the double layer. [c] Determined by extrapolation of the heterogeneous kinetics from a second order polynomial fit. Estimated error of ±0.5 from digital simulation. [d] $\Delta G_o^{\neq}$ determined from the slope of α_{app} *vs.* E plots and $\Delta G_o^{\neq} = F/[8(d\alpha/dE)]$. [e] Based on empirical relationship $\lambda_{het} = 55.7/r_{AB}$. The radii r_{AB} was calculated from the Stokes-Einstein equation and diffusion coefficients to be 3.6, 3.7, 4.6 and 4.2 Å for **1**–**4**, respectively. The effective radius were calculated using $r_{eff} = r_B(2r_{AB} - r_B)/r_{AB}$ to give 2.8, 2.8, 3.0 and 2.9 Å for **1**–**4**, respectively. [f] BDE = $4\Delta G_o^{\neq} - \lambda_{het}$. [g] Based on scan rates between 1.0 and 20 V s^{-1} while all others between 0.1 and 20 V s^{-1}. [h] Corrected for inner reorganization energy of up to 9 kcal mol^{-1} [19]. [i] Corrected for inner reorganization energy of 4 kcal mol^{-1}.

Scheme 1 depicts the heterogeneous ET reduction mechanism of **4** to yield the *cis*-diol. A near quantitative yield of 1,3-diphenylcyclopentene-*cis*-1,3-diol (**4d**) was obtained in 90% yield. The reduction is initiated by DET to the σ* orbital mainly localized on the O-O bond, resulting in homogeneous cleavage and the formation of the distonic radical-anion **4a** with a negative charge on one oxygen atom and an unpaired electron on the other. The distonic radical anion can then subsequently react in one of two ways to yield the *cis*-diol **4d**. Either **4a** generated at the interface of the electrode, could be reduced to the dialkoxide **4b** before diffusing away from the electrode, followed by protonation in the reaction solution or upon work-up to yield **4d**. Alternatively, notably in

the presence of a weak acid, **4a** could be protonated resulting in the alkoxyl radical **4c**, which could be further reduced by the electrode and subsequently protonated to yield **4d**. At a potential of −1.5 V, the reduction of both **4a** and **4c** are predicted to be thermodynamically favorable by at least 25 kcal mol^{-1}.

Scheme 1. The predominant mechanistic pathways to 1,3-diphenylcyclopentene-1,3-*cis*-diol (**4d**) on reduction of the bicyclic endoperoxide **4** with a rotating disc glassy carbon electrode.

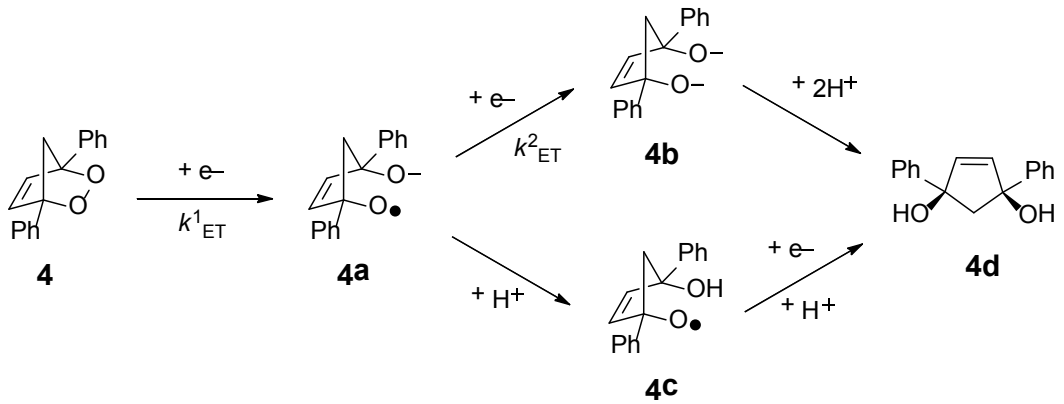

A summary of the thermochemical parameters determined by convolution potential sweep voltammetry are shown in Table 2. The $E°_{diss}$ is related to the O-O bond dissociation energy (BDE) by the equation $E°_{diss} = E°_{\bullet ORRO^-} - BDFE/F$ derived from a thermochemical cycle where $E°_{\bullet ORRO^-}$ is the standard reduction potential of the distonic radical anion, F is Faraday's constant and the BDFE is the bond dissociation free energy, which is the BDE corrected for entropy (BDFE = BDE − $T\Delta S$). The $E°_{\bullet ORRO^-}$ was approximated from the standard potential of the cumyl alkoxyl radical equal to −0.12 V [11]. Using the above equation, the BDFE of **4** is 10 kcal mol^{-1} consistent with previous calculations for the related diphenyl-substituted endoperoxide series [18,19]. The BDE was determined using Savéant's concerted dissociative ET model [31] from the experimental $\Delta G_o^{\neq}$ and the expression $\Delta G_o^{\neq} = (\lambda_{het} + BDE)/4$, where λ_{het} is the solvent reorganization energy. The empirical relation $\lambda_{het} = 55.7/r_{AB}$, was used where r_{AB} is the molecular radius, given in angstroms, as determined from the Stokes-Einstein equation and the experimentally determined diffusion coefficient. An effective radius approach was used in the calculations (see Table 2 footnotes). The r_{eff} was estimated to be 2.9 Å and leading to λ_{het} equal to 19 kcal mol^{-1} and a BDE of 23 kcal mol^{-1}. The slightly higher BDE compared to **1** and **3** is suggestive of a contribution from the relief of ring strain upon fragmentation of the O-O within the bicyclo[2.2.1]hept-5-ene structure. Endoperoxide **3** was estimated to have an inner reorganization energy of 9 kcal mol^{-1} [19]. Following the same approach, **4** has an inner reorganization energy of 4 kcal mol^{-1}.

A final comparison of the kinetic and thermodynamic parameters of **4** with **1** and **2** and **3** is worthy of remarks (Table 2). The $k°_{het}$ and $E°_{diss}$ are identical within experimental error. The diffusion coefficients of **3** and **4** are slightly smaller than **1** and **2** due to the fact that the carbon skeleton is one carbon less and hence the molecular sphere radii are smaller. Using digital simulation, the extracted data from the convolution analysis was adequately reproduced using the experimental cyclic voltammograms of **4** taking into account the lower 1.7 electron stoichiometry by decreasing the initial concentration by 15%. This finding suggests the rapid fragmentation of the distonic radical anion may be producing a species not easily reduced at an electrode potential greater than −2.0 V.

3. Experimental Section

3.1. General Information

N,N-Dimethylformamide (DMF) was distilled over CaH_2 under a nitrogen atmosphere at reduced pressure. Tetraethylammonium perchlorate (TEAP) was recrystallized three times from ethanol and stored in a vacuum oven. Other solvents and reagents not specified were used without purification. Melting points were recorded on an Electrothermal 9100 capillary melting point apparatus and were corrected. UV-visible spectra were recorded on a Varian Cary 100 Bio UV-visible spectrometer. Infrared spectra were recorded on a Bruker Vector 33 FT-IR spectrometer on NaCl plates or in a solution cell and are reported in cm^{-1}. ^1H and ^{13}C-NMR spectra were recorded at 400.1 and 100.6 MHz, respectively, with $CDCl_3$ as the solvent, on a Varian Mercury spectrometer and are reported in ppm. *versus* tetramethylsilane (δ_H = 0.00) for ^1H-NMR and $CDCl_3$ (δ_C = 77.00) for ^{13}C-NMR. Mass spectrometry was performed on a MAT 8200 Finnigan high-resolution mass spectrometer by electron impact (EI) and by chemical ionisation (CI) with isobutane.

3.2. Synthesis of 1,4-Diphenyl-2,3-dioxabicyclo[2.2.1]hept-5-ene (**4**)

The endoperoxide was synthesised by photo-oxygenation of 1,4-diphenyl-1,3-cyclopentadiene as previously described [8]. The reaction was monitored by TLC following the disappearance under 365 nm UV light of the diene at R_f = 0.70 (1:1 hexanes/dichloromethane eluent). The product was purified by flash chromatography using 1:4 hexanes/dichloromethane and collected as the second eluant. The product was recrystallised from MeOH to yield white crystals. m.p. 105–107 °C; ν_{max} (NaCl)/cm^{-1}: 3061, 3033, 2920, 2851, 1700, 1652, 1448, 1333, 1093, 1074, 1025, 887, 823, 749, 697; ^1H-NMR ($CDCl_3$, 400 MHz, ppm): δ_H 2.57 (AB, J = 8.6 Hz, 1H), 2.68 (AB, J = 8.6 Hz, 1H), 6.83 (s, 2H), 7.38–7.48 (m, 6H), 7.56–7.61 (m, 4H); ^{13}C-NMR ($CDCl_3$, 100 MHz, ppm): δ_C 61.12, 96.14, 126.88, 128.78, 129.12, 133.28, 137.89; MS *m/z* (% intensity): 250 ($M^{\bullet+}$, 1) 249 (3), 220 (4), 219 (18), 218 (100), 217 (15), 215 (5), 203 (8), 202 (6), 105 (9), 77 (13); Exact Mass ($M^{\bullet+}$−1): 249.0909 (calculated 249.0915).

3.3. Electrochemistry

Cyclic voltammetry was performed using either a Perkin-Elmer PAR 283 or 263A potentiostat interfaced to a personal computer equipped with PAR 270 electrochemistry software. The working electrode was a 3 mm diameter glassy carbon rod (GC-20, Tokai) sealed in glass tubing. The counter electrode was a 1 cm^2 Pt plate. The reference electrode was a silver wire immersed in a glass tube with a sintered end containing 0.10 M TEAP in DMF. The reference electrode was calibrated against the ferrocene/ferrocenium redox couple after each experiment (0.475 V versus KCl saturated calomel electrode in DMF). Constant potential electrolyses were conducted with a 12 mm tipped glassy carbon rotating disk electrode (EDI101) with a CTV101 speed control unit from Radiometer Analytical [18].

3.4. Heterogeneous Electrolysis Products

1,4-Diphenyl-cyclopent-2-ene-*cis*-1,3-diol was recovered in 90% yield from the electrolysis of 1,4-diphenyl-2,3-dioxabicyclo[2.2.1]-hept-5-ene. ^1H-NMR ($CDCl_3$, ppm): δ_H 2.48 (AB, J = 14.2 Hz, 1H),

2.61 (AB, J = 14.2 Hz, 1H), 2.83 (s, br, 2H), 6.32 (s, 2H), 7.25–7.30 (m, 2H), 7.33–7.40 (m, 4H), 7.44–7.48 (m, 4H), alcohol peak verified by deuterium exchange; ^{13}C-NMR ($CDCl_3$, ppm): δ_C 58.95, 85.90, 124.94, 127.36, 128.42, 140.19, 144.80; MS *m/z* (% intensity): 253 ($M^{\bullet+}$+1,15), 252 ($M^{\bullet+}$,76), 235 (11), 234 (39), 233 (32), 205 (13), 133 (70), 120 (100), 105 (95), 91 (24), 47 (77); Exact Mass: 252.1142 (calculated 252.1150).

4. Conclusions

The bicyclic endoperoxide 1,4-diphenyl-2,3-dioxabicyclo[2.2.1]hept-5-ene (**4**) was studied using heterogeneous electrochemical techniques. It was found that reduction of the O-O bond occurs by a DET mechanism with thermodynamic and kinetic parameters consistent with the other diphenyl-substituted endoperoxides **1**–**3** [18,19]. In all cases, the electrode kinetics are slow and the O-O bond energy is low. This study suggests **4** reacts by a radical-anion chain mechanism initiated by the concerted DET reduction. The overall reactivity of **4** has many characteristics similar to **2** and **3** rather than a clear two-electron mechanism resulting in quantitative formation of *cis*-diol as with **1**. The elucidation of the complete reductive mechanism of **4** is subject to further investigation.

Acknowledgments

This work was financially supported by the Natural Sciences and Engineering Research Council of Canada, the Government of Ontario (PREA) and the University of Western Ontario. Doug Hairsine is acknowledged for performing the mass spectroscopic measurements. DCM thanks the Ontario Government for an OGSST postgraduate scholarship. The University of Malta is acknowledged for continued support.

Author Contributions

D.C.M. conducted the synthesis, electrochemistry, data analysis and wrote the paper. M.S.W. designed the research, analyzed the data and edited the manuscript. The work was originally reported in the Ph.D. dissertation, 2004, by D.C.M. at the University of Western Ontario under the supervision of M.S.W.

Conflicts of Interest

The authors declare no conflict of interest.

References

1. Todres, Z.V. *Organic Ion Radicals: Chemistry and Applications*; Marcel Dekker: New York, NY, USA, 2003.
2. Chatgilialoglu, C.; Studer, A. *Encyclopedia of Radicals in Chemistry, Biology and Materials*; John Wiley & Sons, Inc.: Chichester, UK, 2012.
3. Zhang, N.; Shampa, R.; Rosen, B.M.; Percec, V. Single electron transfer in radical ion and radical-mediated organic, materials and polymer synthesis. *Chem. Rev*. **2014**, *114*, 5848–5958.

4. Stevenson, J.P.; Jackson, W.F.; Tanko, J.M. Cyclopropylcarbinyl-type ring openings. Reconciling the chemistry of neutral radicals and radical anions. *J. Am. Chem. Soc*. **2002**, *124*, 4271–4281.
5. Tanko, J.M.; Phillips, J.P. Rearrangements of radical ions: What it means to be both a radical and an ion. *J. Am. Chem. Soc.* **1999**, *121*, 6078–6079.
6. Chahma, M.; Li, X.; Phillips, P.; Schwartz, P.; Brammer, L.E.; Wang, Y.; Tanko, J.M. Activation/driving force relationships for cyclopropylcarbinyl-homoallyl-type rearrangements of radical anions. *J. Phys. Chem. A* **2005**, *109*, 3372–3382.
7. Tanko, J.M.; Li, X.; Chahma, M.; Jackson, W.F.; Spencer, J.N. Cyclopropyl conjugation and ketyl anions: When do things begin to fall apart? *J. Am. Chem. Soc.* **2007**, *129*, 4181–4192.
8. Gryn'ova, G.; Marshall, D.L.; Blanksby, S.J.; Coote, M.L. Switching radical stability by pH-induced orbital conversion. *Nat. Chem*. **2013**, *5*, 474–481.
9. Gryn'ova, G.; Coote, M.L. Origin and scope of long-range stabilizing interactions and associated SOMO-HOMO conversion in distonic radical anions. *J. Am. Chem. Soc.* **2014**, *135*, 15392–15403.
10. Magri, D.C.; Workentin, M.S. Model dialkyl peroxides of the Fenton mechanistic probe 2-methyl-1-phenyl-2-propyl hydroperoxide (MPPH): Kinetic probes for dissociative electron transfer. *Org. Biomol. Chem.* **2003**, *1*, 3418–3429.
11. Donkers, R.L.; Maran, F.; Wayner, D.D.M.; Workentin, M.S. Kinetics of the reduction of dialkyl peroxides. New insights into the dynamics of dissociative electron transfer. *J. Am. Chem. Soc.* **1999**, *121*, 7239–7248.
12. Antonello, S.; Musumeci, M.; Wayner, D.D.M.; Maran, F. Electroreduction of dialkyl peroxides. Activation-driving force relationships and bond dissociation free energies. *J. Am. Chem. Soc.* **1997**, *119*, 9541–9549.
13. Workentin, M.S.; Maran, F.; Wayner, D.D.M. Reduction of di-*tert*-butyl peroxide—Evidence for nonadiabatic dissociative electron transfer. *J. Am. Chem. Soc.* **1995**, *117*, 2120–2121.
14. Antonello, S.; Formaggio, F.; Moretto, A.; Toniolo, C.; Maran, F. Intramolecular, intermolecular, and heterogeneous nonadiabatic dissociative electron transfer to peresters. *J. Am. Chem. Soc.* **2001**, *123*, 9577–9584.
15. Antonello, S.; Maran, F. The role and relevance of the transfer coefficient alpha in the study of dissociative electron transfers: Concepts and examples from the electroreduction of perbenzoates. *J. Am. Chem. Soc.* **1999**, *121*, 9668–9676.
16. Antonello, S.; Maran, F. Evidence for the transition between concerted and stepwise heterogeneous electron transfer bond fragmentation mechanisms. *J. Am. Chem. Soc.* **1997**, *119*, 12595–12600.
17. Antonello, S.; Crisma, M.; Formaggio, F.; Moretto, A.; Taddei, F.; Toniolo, C.; Maran, F. Insights into the free-energy dependence of intramolecular dissociative electron transfers. *J. Am. Chem. Soc.* **2002**, *124*, 11503–11513.
18. Magri, D.C.; Workentin, M.S. A Radical-anion chain mechanism initiated by dissociative electron transfer to a bicyclic endoperoxide: Insight into the fragmentation chemistry of neutral biradicals and distonic radical anions. *Chem. Eur. J.* **2008**, *14*, 1698–1709.

19. Magri, D.C.; Workentin, M.S. A radical-anion chain mechanism following dissociative electron transfer reduction of the model prostaglandin endoperoxide, 1,4-diphenyl-2,3-dioxabicyclo[2.2.1]heptane. *Org. Biomol. Chem.* **2008**, *18*, 3354–3361.
20. Stringle, D.L.B.; Magri, D.C.; Workentin, M.S. Efficient homogeneous radical-anion chain reactions initiated by dissociative electron transfer to 3,3,6,6-tetraaryl-1,2-dioxanes. *Chem. Eur. J.* **2010**, *16*, 178–188.
21. Donkers, R.L.; Workentin, M.S. Elucidation of the electron transfer reduction mechanism of anthracene endoperoxides. *J. Am. Chem. Soc.* **2004**, *126*, 1688–1698.
22. Donkers, R.L.; Workentin, M.S. Kinetics of dissociative electron transfer to ascaridole and dihydroascaridole—Model bicyclic endoperoxides of biological relevance. *Chem. Eur. J.* **2001**, *7*, 4012–4020.
23. Donkers, R.L.; Workentin, M.S. First determination of the standard potential for the dissociative reduction of the antimalarial agent artemisinin. *J. Phys. Chem. B* **1998**, *102*, 4061–4063.
24. Najjar, F.; André-Barrès, C.; Lacaze-Dufaure, C.; Magri, D.C.; Workentin, M.S.; Tzèdakis, T. Electrochemical reduction of G3-factor endoperoxide and its methyl ether: Evidence for a competition between concerted and stepwise dissociative electron transfer. *Chem. Eur. J.* **2007**, *13*, 1174–1179.
25. Costentin, C.; Hajj, V.; Robert, M. Savéant, J.-M.; Tard, C. Concerted heavy-atom bond cleavage and proton and electron transfers illustrated by proton-assisted reductive cleavage of an O-O bond. *Proc. Natl. Acad. Sci. USA* **2011**, *108*, 8559–8564.
26. Magri, D.C.; Workentin, M.S. Kinetics of the photoinduced dissociative reduction of the Model alkyl peroxides di-*tert*-butyl peroxide and ascaridole. *Mediterr. J. Chem.* **2012**, *6*, 303–315.
27. Magri, D.C.; Donkers, R.L.; Workentin, M.S. Kinetics of the photoinduced electron transfer dissociative reduction of the antimalarial endoperoxide, artemisinin. *J. Photochem. Photobio. A Chem.* **2001**, *138*, 29–34.
28. Costentin, C.; Robert, M. Savéant, J.-M.; Tard, C. Breaking bonds with electrons and protons. Models and examples. *Acc. Chem. Res.* **2014**, *47*, 271–280.
29. Houmam, A. Electron transfer initiated reactions: Bond formation and bond dissociation. *Chem. Rev*. **2008**, *108*, 2180–2237.
30. Costentin, C.; Robert, M.; Savéant, J.-M. Electron transfer and bond breaking: Recent advances. *Chem. Phys*. **2006**, *324*, 40–56.
31. Savéant, J.-M. Electron transfer, bond breaking and bond formation. In *Advances in Physical Organic Chemistry*; Tidwell, T.T., Ed.; Academic Press: New York, NY, USA, 2000; Volume 35, pp. 117–192.
32. Savéant, J.-M. Electron transfer, bond breaking and bond formation. *Acc. Chem. Res.* **1993**, *26*, 455–461.
33. Maran, F.; Wayner, D.D.M.; Workentin, M.S. Kinetics and mechanism of the dissociative reduction of C-X and X-X Bonds (X = O, S). In *Advances in Physical Organic Chemistry*, Tidwell, T.T., Ed.; Academic Press, New York, NY, USA, 2001; Volume 36, p. 85.
34. Imbeaux, J.C.; Savéant, J.-M. Convolutive Potential Sweep Voltammetry: I. Introduction. *J. Electroanal. Chem.* **1973**, *44*, 169–187.

35. Bard, A.J.; Faulkner, L.R. *Electrochemical Methods, Fundamentals and Applications*, 2nd ed.; Wiley: New York, NY, USA, 2001.

Sample Availability: Samples of the compounds **1**–**4** are available from the authors on request.

© 2014 by the authors; licensee MDPI, Basel, Switzerland. This article is an open access article distributed under the terms and conditions of the Creative Commons Attribution license (http://creativecommons.org/licenses/by/3.0/).